halide mixed-ligand clusters B_nX_n and their fragmentation products, while the mass spectra from the B_2Cl_4/CBr_4 reaction were dominated by M - X and M - BX_3 ions from the mixed-halide $C(BX_2)_4$ species. At 97 °C. The ^{11}B NMR chemical shifts of the last compounds range from 51 to 59 ppm;[10] see, for example, Figure 2.

The tetrakis(dihaloboryl)methanes are thought to be formed from the carbon tetrahalides by means of sequential BX insertions. The separation and further study of the tetrakis(dihaloboryl)-methanes like $C(BBrCl)_4$ have been hampered by the fact that while they appear to be reasonably enduring at ambient temperature in boron trihalide solvents, once the boron trihalide has been removed they begin to decompose. Stone[25] has isolated $C(BCl_2)_4$ ($\delta(^{11}B)$ 57.2 ppm) and shown that it is more stable than the less substituted (dichloroboryl)methanes in that it persists at ambient temperature for extended periods. Tetrakis(dichloroboryl)methane was retained at 0 °C on a low-temperature fractionating column, and no molecular ions were observed in the mass spectrum.[25] Aside from the base peaks, the BCl_2^+ ions, the most abundant peaks in the spectrum were derived from the M - BCl_3 ions.[25] These properties, of course, are all consistent with the properties of the $C(BX_2)_4$ compounds observed here.

Overall, the simplest explanation of the currently available data is that the diboron tetrahalides are "stabilized" in haloalkane solutions by equilibria that involve the formation of dihaloboryl ligands from carbon-halogen bonds.[26] The (dihaloboryl)methanes formed, however, are only of moderate stability; thus they act as chemical intermediates, usually regenerating B_2X_4 species by reaction with boron trihalide. Ultimately, however, the much more stable larger polyhedral boron halides and $C(BX_2)_4$ are slowly formed. Under the conditions employed here, the cage compounds are largely the polyhedral boron halides, although small amounts of perhalocarboranes are also generated. Whether the reported stabilization of the diboron tetrahalides by haloalkenes occurs by means of a similar series of reactions or by means of the π complexes previously postulated[4] is currently under investigation.

Acknowledgment. The financial assistance of the National Science Foundation is gratefully acknowledged.

Registry No. $H_2C{=}CH_2$, 74-85-1; B_2Br_4, 14355-29-4; $Br_2B(CH_2)_2BBr_2$, 88870-82-0; $Cl_2B(CH_2)_2BCl_2$, 20816-71-1; BBr_3, 10294-33-4; CBr_4, 558-13-4; CCl_4, 56-23-5; Cl_2BBCl_2, 13701-67-2.

(26) A radical mechanism is thought to be much less probable than that proposed here, in part because as yet we have no mass spectral or ^{13}C NMR evidence consistent with the presence of, e.g., C_2Cl_6 ($\delta(^{13}C)$ 88 ppm), which would be expected to form in chain termination reactions like $2\,{}^{\bullet}CCl_3 \rightarrow C_2Cl_6$.

Notes

Contribution from the Department of Chemistry, University of Illinois at Chicago, Chicago, Illinois 60680

Magnetochemistry of the Tetrahaloferrate(III) Ions. 4. Heat Capacity and Magnetic Ordering in Bis[4-chloropyridinium tetrachloroferrate(III)]-4-Chloropyridinium Chloride

Roey Shaviv and Richard L. Carlin*

Received May 29, 1991

Introduction

The heat capacity of bis[4-bromopyridinium tetrachloroferrate(III)]-4-bromopyridinium chloride, $[4\text{-Br(py)H}]_3Fe_2Cl_9$, was recently presented[1] as part of a comprehensive study of the magnetochemistry of the tetrahaloferrates(III). These compounds are found to be canted antiferromagnets in which the character of the long-range magnetic ordering is dependent on both the nature of the anion $[FeX_4]^-$ (X = Cl, Br, or a mixture of the two) and on chemical substitution in the cation $[4\text{-X(py)H}]^+$ (X = H, Cl, or Br).[2-6] Canted antiferromagnets of iron(III) are not very common, and the systematic rules for their preparation are not at all clear.[7]

The title compound, $[4\text{-Cl(py)H}]_3Fe_2Cl_9$, and its chemical relative $[4\text{-Br(py)H}]_3Fe_2Cl_9$ are isostructural and both undergo long-range magnetic ordering between 2 and 3 K.[2,3] The small difference in the ordering temperatures is due to the chemical substitution, for the substitution of chlorine for bromine makes the cation somewhat smaller without a change in the structure. The iron-iron distance is therefore reduced, and magnetic exchange becomes larger. The critical temperature increases from 2.29 K to 2.69 K upon replacement of the 4-bromo cation with the 4-chloro one. The large cation also enhances short-range interactions since the tetrahaloferrate(III) ions are paired and these pairs are somewhat isolated from each other. Thus, the magnetic heat capacity of $[4\text{-Br(py)H}]_3Fe_2Cl_9$ displays a λ-type phase transition at the critical temperature and an additional broad peak associated with the pairwise short-range ordering phenomenon.[1]

Experimental Section

Single crystals of $[4\text{-Cl(py)H}]_3Fe_2Cl_9$ were synthesized by a procedure that was previously described.[2,3] The single crystals were crushed and pelleted for this experiment. The sample pellet was threaded with about 0.3 g of fine copper wire in order to facilitate rapid thermal equilibrium. To establish thermal contact between the sample pellet and the calorimeter, 0.24 g of Apiezon N grease was spread on the interior of the calorimeter. The mass of the sample was 8.46767 g. Chemical analysis and structural data were previously presented.[2,3]

The heat-capacity measurements were conducted in the adiabatic calorimetric cryostat that is described elsewhere.[1] The pelleted sample was contained in a gold-plated copper calorimeter whose mass was about 6.0 g and whose heat capacity was determined in a separate experiment. Measurements were conducted using the heat-pulse technique. The precision of a single point, which is dependent on the temperature and more importantly on the temperature increments (since $C_p = (\Delta H/\Delta T)$ when C_p is the apparent heat capacity and ΔH and ΔT are the energy input and the temperature change, respectively) is less than 0.1% outside of the transition region. In the transition region where temperature increments were typically less than 0.05 K the experimental precision is somewhat reduced (for the benefit of greater resolution) and the precision of a single point is about 1%. The heat capacity of the empty calorimeter represented no more than 5% of the total heat capacity throughout the experimental region.

Results and Discussion

The molar heat capacity of bis[4-chloropyridinium tetrachloroferrate(III)]-4-chloropyridinium chloride is plotted in Figure 1a,b. A λ-type phase transition associated with the long-range ordering is found at 2.685 K, which may be identified as the critical temperature.

The heat capacity is assumed to consist of lattice and excess contributions. The lattice contribution is the heat capacity due to thermal activation of lattice vibrations when the harmonic

(1) Shaviv, R.; Merabet, K. E.; Shum, D. P.; Lowe, C. B.; Gonzalez, D.; Burriel, R.; Carlin, R. L. *Inorg. Chem.*, in press.
(2) Lowe, C. B. Thesis, University of Illinois at Chicago, 1990.
(3) Zora, J. A.; Seddon, K. R.; Hitchcock, P. B.; Lowe, C. B.; Shum, D. P.; Carlin, R. L. *Inorg. Chem.* **1990**, *29*, 3302.
(4) Lowe, C. B.; Carlin, R. L.; Schultz, A. J.; Loong, C.-K. *Inorg. Chem.* **1990**, *29*, 3308.
(5) Carlin, R. L.; Lowe, C. B.; Palacio, F. *An. Quim.* **1991**, *87*, 5.
(6) Shaviv, R.; Lowe, C. B.; Carlin, R. L. To be published.
(7) Carlin, R. L. *Magnetochemistry*; Springer-Verlag, Berlin, 1986.

0020-1669/92/1331-0710$03.00/0

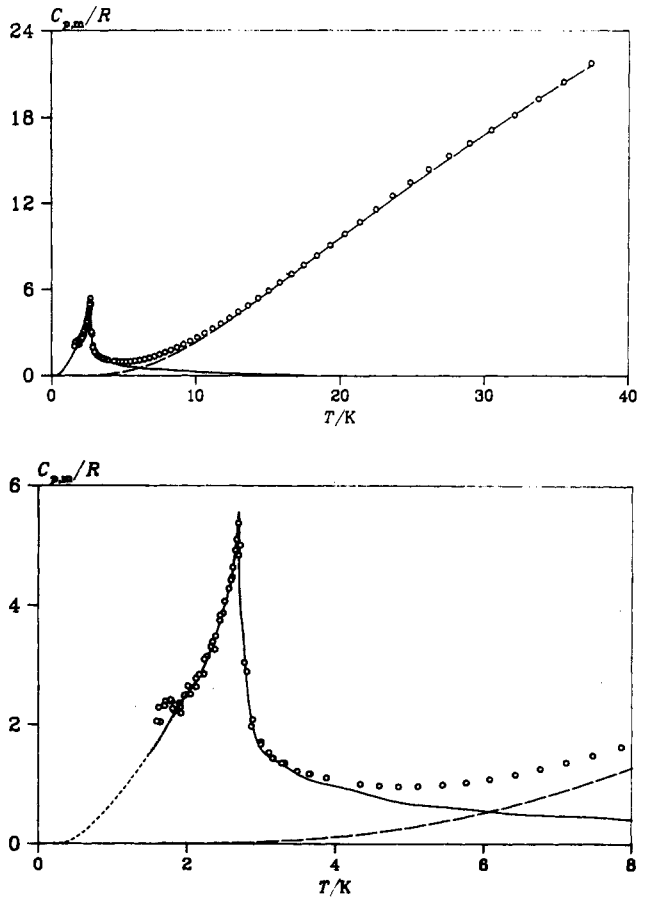

Figure 1. (a) Top: Molar heat capacity of $[4\text{-Cl(py)H}]_3Fe_2Cl_9$. Key: O, experimental points; ---, lattice contribution; - - -, excess (magnetic) heat capacity; ···, extrapolation of the data to 0 K. (b) Bottom: Transition region on a magnified scale.

(adiabatic) approximation is assumed. The excess heat capacity is defined as all contributions other than the lattice contribution and in the present context is the magnetic heat capacity. Since the experimental result consists of a sum of the lattice and magnetic contributions, a reliable method to separate the two is in order.

The lattice heat capacity was determined by means of the enhanced Komada/Westrum phonon distribution model[8] in a manner similar to that described in the preceding paper in this series.[1] The method approximates the phonon density of states on the basis of the experimental heat capacity and several physical parameters related to the mass and structure of the compound in question. The calculated density of states function is in turn represented by the single output parameter—the apparent characteristic temperature—Θ_{KW}. An apparent characteristic temperature, Θ_{KW}, which is independent of temperature indicates that the experimental heat capacity may be reproduced by a single phonon distribution function over an extended temperature region. When excess heat capacity is extant, Θ_{KW} tends to decrease in value. Phase transitions typically result in a minimum in the apparent characteristic temperature. The calculated quantity Θ_{KW} for $[4\text{-Cl(py)H}]_3Fe_2Cl_9$ is presented in Figure 2. Once Θ_{KW} was calculated, the lattice heat capacity was easily obtained (Figure 1a,b).

The lattice heat capacity curve is observed to have an inflection point in the vicinity of 18 K and is concave toward the abscissa above that temperature and displays what may appear to be a broad hump. This abnormally low inflection point in the heat capacity and the apparent hump that follows are believed to be due to the thermal activation of low-lying vibrational modes associated with librations of the organic groups and is typical of other

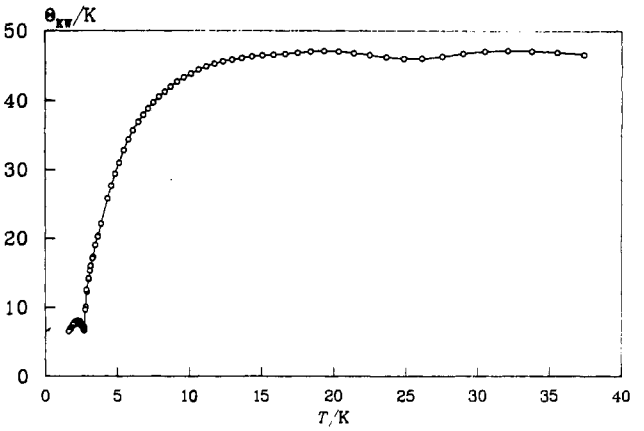

Figure 2. Apparent characteristic temperature Θ_{KW} for $[4\text{-Cl(py)H}]_3Fe_2Cl_9$ between 1.5 and 40 K.

materials in this chemical system.[1,6] The heat capacity associated with these librations was approximated by two weighted Einstein functions, at 38 and 72 K, incorporated into the phonon density of states function as internal modes. The lattice heat capacity thus produced is in excellent agreement with the experimental heat capacity above 17.5 K, indicating that no excess contributions to the heat capacity are present above that temperature.

The absence of excess heat capacity above 17.5 K stands in sharp contrast to what is observed with $[4\text{-Br(py)H}]_3Fe_2Cl_9$, in which pairwise interactions give rise to a magnetic contribution which reaches its maximum at about 21 K, corresponding to an exchange constant $J'/k_B = -26.7$ K for the intradimer interaction.[1] It is apparent that the change in cation size allows for long-range exchange, which is now the dominant interaction at the expense of short-range pairwise ordering. Evidently, the dimer interactions are controlled by the nature of the cation and thus chemical substitution may provide a switch able to turn these interactions on and off.

Once the lattice heat capacity is determined, the magnetic heat capacity may be evaluated and analyzed. The heat capacity in the transition region is presented in Figure 1b. Four functions are displayed in the figure. These are the experimental and the lattice heat capacities, the excess heat capacity, which is the difference between the lattice and the experimental heat capacities, and the curve used to extrapolate the excess heat capacity to 0 K. A physically significant extrapolation is important if a correct interpretation of the transitional heat capacity is to be obtained. Thus, the excess heat capacity, up to 3.4 K, was used to calculate a distribution function, which was, in turn, used to extrapolate the experimental results to 0 K. Several constraints were placed on the extrapolation: (a) a T^3 dependence of the curve at very low temperatures;[9] (b) a smooth junction with the experimental results and a good agreement with them up to 2.0 K; (c) agreement of the resulting entropy with theoretical predictions. Noteworthy is the fact that several experimental points below 1.8 K show higher than expected heat capacity. This phenomenon is probably due to impurities and to poorer adiabatic conditions below 1.8 K, which results in lower precision below that temperature.

Once the extrapolation of the excess heat capacity to 0 K is achieved, the magnetic heat capacity is fitted to two polynomials and integrated between 0 and 17.5 K. The entropy of disorder, $\Delta_{tr}S_m^\circ$, as found from this integration is $3.565R$, which is 0.5% smaller than the theoretical value for a $S = {}^5/_2$ system, $2 \ln 6 = 3.584R$ [there are two iron(III) ions in a formula unit]. The transition temperature is identified at 2.685 ± 0.01 K with a corresponding heat capacity and critical entropy of $5.558R$ and $2.336R$, respectively. About two-thirds of the disorder process is completed below the critical temperature, as indicated by the entropy values. By comparison only about 50% of the disorder process in $[4\text{-Br(py)H}]_3Fe_2Cl_9$ takes place below the transition

(8) Komada, N.; Westrum, E. F. *Thermochim. Acta* **1988**, *109*, 11.

(9) Cracknell, A. P.; Tooke, A. O. *Contemp. Phys.* **1979**, *20*, 55.

temperature. Short-range order effects play a much smaller role in the magnetic interactions of $[4\text{-Cl(py)H}]_3Fe_2Cl_9$ relative to those in $[4\text{-Br(py)H}]_3Fe_2Cl_9$.

The magnetic ordering temperature, 2.685 K, is lower than the value 2.73 K obtained by susceptibility measurements. This discrepancy is insignificant. The effects of the high pressure required for pelleting the sample are a likely source for the shift in the critical temperature.

The exchange constant J/k_B may be obtained from the tail of the heat capacity in the post transition region which follows the relation[7]

$$C_{p,ex}/R = 2[S(S+1)]^2 z J^2/3k_B^2T^2$$

where $S = {}^5/_2$ for iron(III) and z is the magnetic coordination number, assumed to be 6 for the present system. A plot of the excess heat capacity against T^{-2} should, therefore, be linear, and J/k_B may easily be obtained from its slope. Such a plot is indeed found to be linear between 2.9 and 4.5 K. The exchange constant, J/k_B, is found to be 0.110 K, in excellent agreement with the values of 0.110, 0.110, and 0.125 K obtained from magnetic susceptibility experiments.[2] The heat capacity is thus found to confirm the susceptibility results, and we conclude that long-range ordering dominates the magnetic interactions in this material.

Acknowledgment. We thank Dr. Carol B. Lowe for supplying the sample. This research was supported by the Solid State Chemistry Program of the Division of Materials Research of the National Science Foundation, under Grant DMR-8815798.

Contribution from the Department of Chemistry, North Dakota State University, Fargo, North Dakota 58105

A Convenient Synthesis of Tricyclo[3.3.1.1^{3,7}]tetrasilathianes and Tricyclo[3.3.1.1^{3,7}]tetrasilaselenanes

Steven R. Bahr and Philip Boudjouk*

Received September 9, 1991

Introduction

There are only two reports describing the synthesis of adamantane-like structures composed of silicon and selenium, $(RSi)_4Se_6$, one which utilizes volatile H_2Se with a trichlorosilane[1] and the other requiring a reaction time of several days between trichlorosilane and hexamethyldisilathiane.[2] Of the few references for synthesizing the silicon–sulfur system, only one gives good yields deriving from $RSiCl_3$ and $(Me_3Si)_2S$.[3] The instability of the Si–S or Si–Se bond toward hydrolysis imposes the requirement of an anhydrous route to these compounds. Recently, we have reported convenient high-yield procedures for making anhydrous Na_2S[4] and Na_2Se[5,6] from sodium, sulfur, or selenium and a catalytic amount of naphthalene in THF as a useful step in preparing a variety of organic and organosilicon chalcogenides. In this note we describe a simple procedure for making silicon–chalcogenide adamantane cage systems on a preparative scale employing our sodium sulfide or sodium selenide that avoids the use of volatile selenides as well as meeting the requirement that the synthesis be anhydrous.

Experimental Section

Materials and General Procedures. Sodium sulfide and sodium selenide were prepared from sulfur or selenium powder, and sodium chips were prepared by cutting pellets. Commercially available trichlorosilanes (Petrarch) were distilled before use. Tetrahydrofuran was distilled from sodium benzophenone ketyl just prior to use. Hexane was stirred over H_2SO_4 and distilled. Benzene was dried by azeotropic removal of water and distilled into a storage bottle. All experiments were performed under a dry-nitrogen atmosphere and air-sensitive compounds were transferred in an argon-filled glovebox.

The ^1H (399.78 MHz), ^{13}C (100.52 MHz), $^{2}19Si$ (79.43 MHz), and ^{77}Se (76.22 MHz) NMR spectra were obtained on a JEOL GSX400 spectrometer. A 5-mm broad-band probe equipped with a variable-temperature accessory controlled the temperature at 25 ± 0.5 °C. Samples were prepared as 20–30% by volume solutions in $CDCl_3$ or C_6D_6. ^1H, ^{13}C, and ^{29}Si chemical shifts are reported in parts per million (ppm) with respect to Me_4Si (0 ppm) while ^{77}Se shifts are reported with respect to a 25% solution of Me_2Se in $CDCl_3$ (0 ppm). ^{29}Si NMR spectra were acquired by using a refocused INEPT pulse sequence. The ^{29}Si chemical shifts were measured from an external reference of 25% Me_4Si in $CDCl_3$. Infrared spectra were recorded on a Mattson Cygnus 25 FT-IR instrument. Elemental analysis was performed by Galbraith Laboratories in Knoxville, TN. Mass spectra were obtained on a MAT CH-5DF or CH7 mass spectrometer at 70 eV. Melting points were taken on a Thomas Hoover capillary melting point apparatus and are uncorrected.

Synthesis of Tetramethyl-, Tetraethyl-, and Tetraphenyltricyclo[3.3.1.1^{3,7}]tetrasilaselenane. The synthesis of $(EtSi)_4Se_6$ (**2**) described below is similar to that used for the methyl and phenyl analogues. A 500-mL reaction flask was equipped with a condenser, a 125-mL addition funnel and charged with sodium chips (2.76 g, 120 mmol), selenium powder (4.68 g, 60 mmol), naphthalene (1.5 g, 12 mmol), and 100 mL of THF. To insure complete consumption of sodium, the mixture was refluxed for 10 h, giving a white suspension of Na_2Se. (If a purple color persists at this point, small amounts of sodium can be added until the white endpoint is attained. For a green mixture, adding Se powder will eventually give the white suspension.) An additional 100 mL of THF was added and $EtSiCl_3$ (6.5 g, 40 mmol) dissolved in 50 mL of THF was placed in the addition funnel while the contents of the flask were cooled to 0 °C. The $EtSiCl_3$ solution was added dropwise over a 1 h period. The reaction mixture turned red after being stirred at room temperature for 12 h and then to tan after 1 day. THF was removed by vacuum, and the salts were removed by adding 100 mL of benzene followed by filtration through a coarse glass frit yielding a yellow liquid. The benzene was removed under reduced pressure, and the remaining light yellow solid was recrystallized in benzene/hexane to yield 2.1 g of **2** as white crystals. The filtrate was concentrated, and an additional 0.6 g was isolated after recrystallization (total yield of **2**: 2.7 g, 40%): mp 171–172 °C (lit.[1] 170–171 °C); ^1H NMR ($CDCl_3$) δ 1.22 (t, 3 H, CH_3), 1.65 (q, 2 H, CH_2); ^{13}C NMR ($CDCl_3$) δ 6.2, 18.9 (CH_2CH_3); ^{29}Si NMR ($CDCl_3$) δ 6.8; ^{77}Se NMR ($CDCl_3$) δ −110. MS: *m/e* 696 (M^+, 6.8%) with correct isotope distribution for six Se atoms.

The above procedure with $MeSiCl_3$ produced **1** as a white crystalline solid after recrystallization in two crops (total yield of **1**: 2.4 g, 37%): mp 280–283 °C (lit.[1] 283–284 °C). ^1H NMR ($CDCl_3$) δ 1.38 (s, CH_3); ^{13}C NMR ($CDCl_3$) δ 11.8; ^{29}Si NMR ($CDCl_3$) δ −0.8; ^{77}Se NMR ($CDCl_3$) δ −81. MS: *m/e* 640 (M^+, 3.9%) with correct isotope distribution for six Se atoms.

A similar procedure using $PhSiCl_3$ gave **3** as white crystals (total yield of **3**: 1.1 g, 12%): mp >270 °C; ^1H NMR (C_6D_6) δ 7.85 (d, 2 H, C_6H_5), 7.45 (m, 3 H, C_6H_5); ^{13}C NMR (C_6D_6) δ 134.8, 133.1, 131.2, 128.8 (C_6H_5); ^{29}Si NMR (C_6D_6) δ −6.1; ^{77}Se NMR (C_6H_6) δ −88. MS: *m/e* 894 (M^+, 3.7%) with correct isotopic distribution for six Se atoms. Anal. Calcd for $C_{24}H_{20}Si_4Se_6$: C, 32.22; H, 2.25. Found: C, 32.21; H, 2.30.

Synthesis of Tetramethyl- and Tetraethyltricyclo[3.3.1.1^{3,7}]tetrasilathiane. A 500-mL 3-necked round-bottomed flask fitted with a condenser/N_2 inlet and a 250-mL addition funnel was charged with sodium chips (5.50 g, 240 mmol), sulfur powder (3.80 g, 120 mmol), naphthalene (3.1 g, 24 mmol), and 200 mL of THF. A gray suspension of Na_2S resulted after 10 h at reflux. This mixture was cooled to 0 °C and treated by dropwise addition of $EtSiCl_3$ (13.1 g, 80 mmol) in 100 mL of THF over a 1-h period. Stirring at room temperature for 15 h gave a light tan mixture. Removal of solvent by vacuum followed by extraction and filtration with 50 mL of benzene gave a yellow solution. The benzene was removed under reduced pressure, naphthalene was removed by sublimation (50 °C, 0.1 Torr), and the remaining yellow solid was recrystallized in hexane to give 4.2 g (50% yield) of $(EtSi)_4S_6$ (**5**) as white crystals: mp 134–137 °C (lit.[7] 140 °C); ^{29}Si NMR ($CDCl_3$) δ 21.9 (lit.[7] δ 21.9).

* To whom correspondence should be addressed.

(1) Forstner, J. A.; Mutterties, E. L. *Inorg. Chem.* **1966**, *5*, 552.
(2) Haas, A.; Hitze, R.; Kruger, C.; Angermund, K. *Z. Naturforsch., B: Anorg. Chem., Org. Chem.* **1984**, *39B*, 890.
(3) Horn, H.-G.; Hemeke, M. *Chem.-Ztg.* **1985**, *109*, 145.
(4) So, J.-H.; Boudjouk, P. *Synthesis* **1989**, 306.
(5) Thompson, D. P.; Boudjouk, P. *J. Chem. Soc., Chem. Commun.* **1987**, 1467.
(6) Thompson, D. P.; Boudjouk, P. *J. Org. Chem.* **1988**, *53*, 2109.
(7) Horn, H.-G.; Hemeke, M. *Chem.-Ztg.* **1982**, *106*, 263.

0020-1669/92/1331-0712$03.00/0